Journal of Engineering and Sustainable Development
Vol. 30, No. 01, January 2026
https://jeasd.uomustansiriyah.edu.iq/index.php/jeasd
ISSN 2520-0917
Research Article
https://doi.org/10.31272/jeasd.2564

Experimental Investigation into The Effects of Rebar Corrosion on The Behavior of Reinforced Concrete Columns

Shaho Mahmoud Hama[1*], Ali Hameed Aziz[2]

[1]Civil Engineering Department, College of Engineering, University of Anbar, Ramadi, Iraq
[2]Civil Engineering Department, College of Engineering, Mustansiriyah University, Baghdad, Iraq

[*]Email: shaho_m83@uoanbar.edu.iq

Article Info

Received	09/04/2024
Revised	05/12/2025
Accepted	11/12/2025

Abstract

The durability of reinforced concrete columns can be compromised by steel bar corrosion, leading to weakening and an inability to withstand design loads. The current research investigates the combined effect of longitudinal and confining reinforcement corrosion on the axial capacity of RC columns. Nine column samples (110 x 110 x 1160 mm) were tested and subjected to an artificial electrical corrosion process to expedite mass loss in both longitudinal steel and tie bars. The columns experienced a significant reduction in ultimate load-bearing capacity due to the weakened bond between the concrete and the reinforcement steel. Corrosion of the reinforcing steel and the formation of iron oxide layers negatively impacted the columns' load capacity. According to the findings, the average crack widths are 0.38 mm at 10% mass loss and 0.49 mm at 20% mass loss, with maximum crack widths ranging from 0.37 mm to 0.64 mm. The ultimate loading capacity decreased by 18.5% to 51% for a 10% mass loss and 25% to 65% for a 20% mass loss compared to the reference column without corrosion.

Keywords: Column, Corrosion, Longitudinal displacement, Mass losses.

1. Introduction

Several negative drawbacks can occur as a result of corrosion in steel-reinforced concrete. One of these drawbacks is a decrease in the reinforcement area and ductility, which can lead to severe deterioration [1], [2]. Corrosion causes steel to expand and produce several byproducts, thereby increasing its volume to six times that of the original steel bar [3]. The internal tensile stress can increase due to corrosion-induced damage to the surrounding concrete. Consequently, the most common physical side effect is delamination of the cover and the development of cracks [4], [5].

Steel bars in concrete typically do not require corrosion protection because the surrounding environment is generally highly alkaline. It can prevent corrosion of steel reinforcements by creating a passive layer of iron oxides at the concrete/steel contact [6]. Steel corrosion can begin when oxygen and water are present near the surface of the metal. The carbonation process of concrete, which lowers the alkalinity and eliminates chlorides from the vicinity of the steel surface, is a key component in preventing steel corrosion in concrete structures. Chloride ions enter concrete through cracks or pores, which starts the corrosion reaction [1].

Therefore, the formation of carbonic acid (H2CO3) occurs as carbon dioxide (CO2) infiltrates the concrete pores from the atmosphere and subsequently dissolves in water. This process is known as concrete carbonation. Afterwards, the acid causes the concrete's alkalinity to drop, which in turn ends the passive layer on the steel bars and signals the start of corrosion [6]. The presence of chlorides, which, when dissolved in the water of pores, can transform into hydrochloric acid, could have a similar effect on lowering the alkalinity of concrete [7]. An electrochemical process in which chemical and electrical processes combine, the function of moving electrons from one location to another, causes steel to corrode in concrete [8]. Corrosion in concrete mimics the appearance of a galvanic cell because of the cathode and anode. As the anode dissolves, the iron surface of the steel bar releases ferrous ions. At other locations on the cathode, the released ions undergo a chemical reaction with water and oxygen, resulting in the formation of hydroxide ions (OH). Ferrous hydroxide can be formed when the anode's ferrous ions and the cathode's hydroxide react. After reacting with water, ferrous hydroxide becomes ferric

hydroxide (Fe(OH)3). Then it undergoes a further transformation into hydrated ferric oxide, a compound that contains both iron and water known as Fe2O3.H2O.

As corrosion advances, the volume affected by corrosion will expand to six times its original size owing to the expansion caused by corrosion and the generation of various byproducts [3]. Therefore, corrosion remnants, such as fissures, present on concrete surfaces increase the rate of corrosion. This is because these residues can create an environment conducive to corrosion, thereby allowing corrosion to progress more rapidly. Corrosion can impact the performance and corrosion rate of one type of reinforcement. Corrosion in stirrups can cause longitudinal bars to buckle and reduce load-carrying capacity. The rust and corrosion products from both types of bars can combine, raising internal tensions in the concrete and resulting in more severe cracking and spalling. As a result, it is important to address any corrosion-related issues on concrete surfaces to avoid additional damage and ensure the longevity of the structure [9]. Researchers examined how corrosion of the reinforcing bars in reinforced concrete columns affected their ability to withstand earthquakes [10]. In 2012, thirteen circular reinforced concrete columns were subjected to accelerated wear tests by Ma et al. [11] and were subsequently tested under a static axial load. The variables controlled during testing were wear level and axial load percentage. When the percentage loss in the deteriorated rebar is below 14%, the test results indicate that corroded samples dissipate nearly as much energy as control samples at the same displacement, irrespective of the level of corrosion. Conversely, higher axial loads and wear levels result in a less stable condition, severe hardness degradation, and reduced ductility. Li et al. [12] conducted an experimental study on the decline in mechanical performance of reinforced concrete (RC) columns with eroded reinforcement under constant loads. This study involved testing ten RC column samples and examining the impact of different levels of continuous load (0%, 30%, and 60% of the final designed loading capacity), reinforcement wear (0%, 5%, 10%, and 20%), last bearing capacity, and axial-axial load. The distortion relationship was analyzed. The results showed that the coupling of adverse effects due to reinforcement of continuous wear and loading greatly exacerbates the mechanical deterioration of RC shafts and leads to failure.

Additional studies examined the effectiveness of RC columns subjected to partial reinforcement corrosion, emphasizing the corrosion length and stress state parameters [13], [14]. Similar contributions can be found in the literature [15], [16]. The majority of the studies mentioned above only consider longitudinal reinforcement corrosion. This is not entirely in line with real-life situations; the corrosion occurs in both the longitudinal reinforcements and the lateral reinforcements. In fact, the thinner concrete cover on the lateral reinforcements often makes them corrode even more severely [17].

RC columns are deemed a crucial structural component in damaged concrete constructions. Concrete deterioration caused by the corrosion of steel reinforcement or lateral reinforcements leads to a decrease in column strength and the inability to support design loads. Reinforcement corrosion in reinforced concrete columns can lead to a substantial decrease in capacity regardless of the impact of steel corrosion on structural durability. The previous study focused on corrosion on either longitudinal or confined reinforced. This work investigated the combined effect of corrosion in longitudinal and confined reinforcements on reinforced column capacity.

2. Materials and Experimental Program

A total of nine columns, with dimensions of (110 x 110 x 1160) mm, were tested using the electrochemical corrosion method to assess mass loss in the longitudinal and tie steel bars. These columns also feature corbels measuring 200 mm in length, 110 mm in width, and 100 mm in height at their ends. These columns were divided into three groups, each comprising three columns: reference, 10% corrosion, and 20% corrosion. The columns were designed according to ACI 318M-19 code [18] and reinforced, in a longitudinal direction by (4ϕ 10 mm) deformed bars with (1120 mm) length, while the ties were (ϕ6 mm @100mm). The reinforced steel bars were tested in accordance with ASTM E615 [19]. Fig. 1 illustrates lubricated plywood molds, and Fig. 2 shows Details of the column reinforcement.

For all specimens' mix, the cement content was (450 kg/m^3), the sand was (675 kg/m^3), the gravel was (1125kg/m^3), and the water/cement ratio was (0.42). Ordinary Portland cement (Type-I) with fineness and specific gravity of 450 m^2/kg and 3.15, respectively, was used to cast all control and column specimens. This cement satisfies the limitation of I.S. No.5/2019 [20].

Natural local sand was used as a fine aggregate, with a fineness modulus of 2.35; the specific gravity, SO3 content, and water absorption were 2.5, 0.15%, and 0.15%, respectively. It may be noted that the sand satisfies the limitation of I.S. No.45/1984 [21]. Crushed stone with a maximum size of 10 mm was used in this work. The specific gravity, SO3%, and water absorption were 2.58, 0.08%, and 0.25%, respectively, and all were within the limits of I.S. No. 45/1984 [21].

The compressive strength was determined by averaging the results of three (150x150x150 mm) cubes tested according to BS1881-116 [22], Fig. 3.

Furthermore, the electrical tape was distorted at the junction of the ties and longitudinal bars. With the insulation removed from the electrical wire, which acts as an anode, any steel exposed to corrosion along its length is rolled by the stripped wire, which acts as an electron acceptor.

Following the curing procedure, six columns measuring 110 x 110 x 1160 mm were subjected to electrolytic corrosion to accelerate the deterioration of the longitudinal and tie bars. Two corrosion grades were used in this study: 10% and 20%. A direct current was applied to longitudinal steel bars and tie bars using a DC power supply to accelerate corrosion. The maximum current that a DC power source can supply is 35 Amps.

Figure 1. Lubricated plywood molds and steel reinforcement.

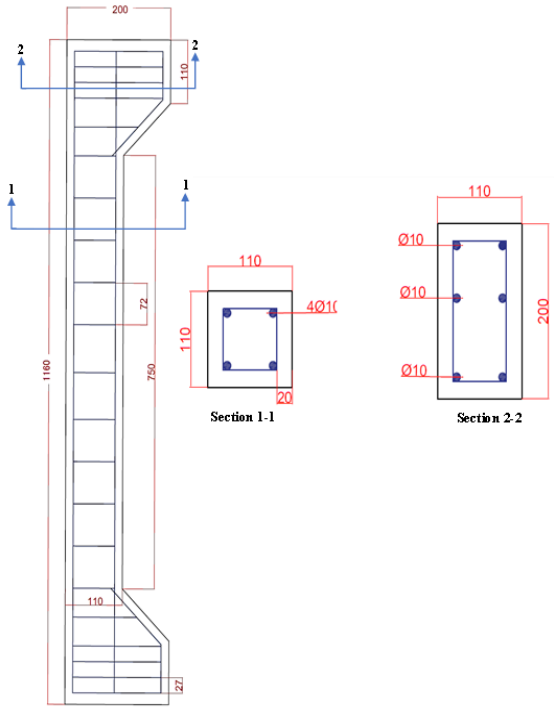

Figure 2. Details of the column reinforcement (dimensions-mm).

Figure 3. Control sample tests.

The specimens were placed on a 100 mm thick wooden support and submerged in a water tank that measured (3800 x 2000 x 800) mm. To prepare the specimens for electrochemical corrosion testing, they were submerged in water containing 5% sodium chloride for 24 hours, with the water level approximately 190 mm above the top of the column. The incorporated long, constrained reinforcements were connected to the positive end of the Direct Current power supply via an electrical cable, serving as the anode. External stainless-steel plates measuring 900 mm in length and 190 mm in height were affixed to the negative end of each specimen to serve as the cathode. The longitudinal reinforcement and stainless-steel plates were attached in the order shown in Fig. 4.

All the longitudinal reinforcement and stirrup steel were interconnected using copper wires, which were subsequently connected to the anode side of the DC power supply. To hasten corrosion, the longitudinal and tie bars were subjected to a current density of 0.2 mA/cm^2 using a direct current (DC) source. In contrast, the theoretical guidance for estimating the time required to induce corrosion damage was provided by Faraday's formula (1).

$$M = A.Time.Se.w/(n.F) \quad (1)$$

Where:

M = Loss of mass (grams)

A = The density of current (milliamperes per square centimeter)

Time = The time it takes for corrosion to occur (seconds)

Se = rusted steel surface area (centimeter^2)

w = The mass of the atomic metal (56 grams for iron, Fe^{+2}) [23].

n = The quantity of iron electrons transmitted during the corrosion process, where n equals 2 for Fe^{+2}.

F = The value of Faraday's constant, as expressed as 96.500 C/equivalent.

Figure 4. Accelerated corrosion setup.

After positioning the column in the testing machine, its vertical alignment was guaranteed. The gadgets were subsequently set up in a circle around the column.

For the linear load simulation, the force was applied over a cylindrical roller. For axial loading of specimens, the force was applied via a supporting device, resulting in a supported column. Load cell readings were obtained at 5.0 kN intervals as the loading was increased until the columns failed. The surfaces of the tested column exhibited cracking. Observable fissures were created in the concrete, and the corresponding loading values were noted. At 0.25L and 0.75L from the column lengths, and in the center, a horizontal LVDT was used to measure the middle height lateral displacement with loads. To measure the axial deformation of the columns under load, a vertical LVDT was attached to the top base of the testing equipment and could be moved from one side to the other (Fig. 5).

To measure the mid-height strain in the longitudinal reinforcement steel under load, a strain gauge with dimensions not exceeding 10 mm × 5 mm was used. The strain gauge was affixed to one side of the reinforcing steel and carefully insulated to prevent corrosion. Because electron transmission and escape from the outer surface of the reinforcing steel pose a corrosion risk, the well-insulated section where the strain gauge was attached will remain free of corrosion, and the gauge will remain reliable throughout the duration of the tests.

3. Results and Discussion

Each bar was connected to a power source via an electrical wire and used as an electrical acceptor to accelerate the corrosion of the steel bars. Faraday's law was used to determine the duration of an accelerating process [24]-[29]. After the corrosion process and structural tests were finished, the steel bars were removed, and their mass loss was assessed. The weight was recorded, and the loss was computed to get the average corrosion level.

Figure 5. Column specimen setup.

If mass loss was between 10% and 20%, it was classified as medium; if it exceeded 20%, it was classified as high. Fig. 6 illustrates the results of mass reduction for all steel bars.

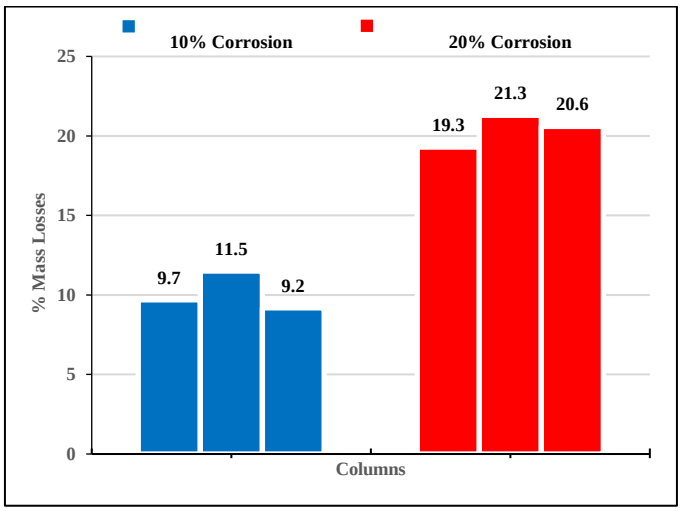

Figure 6. Mass losses due to the corrosion process.

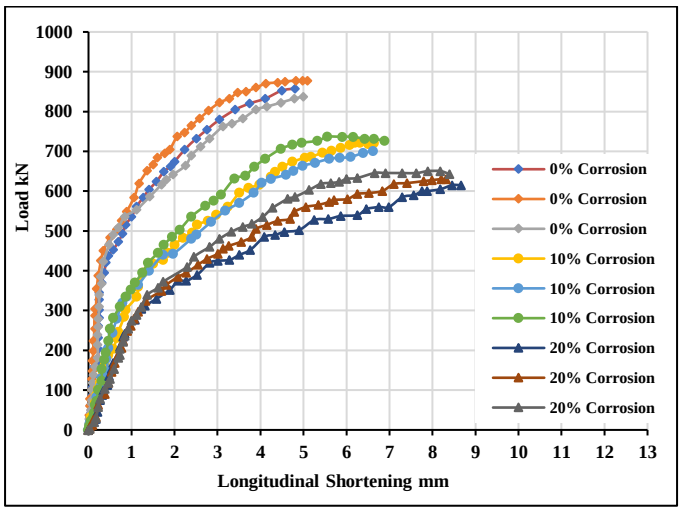

Figure 8. Load-displacement relation for tested columns.

Low stress levels reduce the bond strength of the chemical bonds formed between steel and hardened cement. Radial microcracks in concrete arise from the deterioration of chemical bonds. Fig. 7 depicts the relationship between the average mass reduction of steel bars and the average and maximum cracking widths caused by corrosion on the surface of the concrete cover. The data collected indicate that the average crack width in columns was 0.33 mm at 10% loss and 0.54 mm at 20% loss. Maximum crack widths ranged from 0.37 mm to 0.64 mm for mass loss of 10 % and 20 %, respectively.

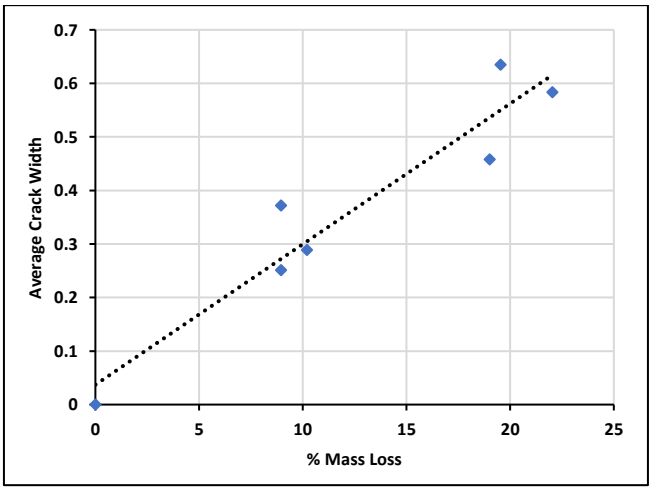

Figure 7. Mass losses vs. average crack width.

The longitudinal shortening-displacement versus load relationships of the tested RC columns are illustrated in Fig. 8.

Displacements were continuously monitored during the test to monitor the growing rate of displacement, which signaled the imminent collapse of the column samples. The decrease in the bond between concrete and reinforcement steel led to a noticeable reduction in the columns' ultimate load capacity.

The decrease occurred when the steel reinforcement corroded, forming an iron oxide coating that reduced the columns' ultimate load capacity. A reduction in maximum load capacity was observed, ranging from 18.5% to 51% for 10% mass loss and from 25% to 65% for 20% mass loss.

Concurrently, the mid-height strain of the longitudinal reinforcement steel was measured during the test, and it was found that the rate of strain increase rose by approximately 31% for a 10% loss in mass and 55% for a 20% loss in mass, as shown in Fig. 9.

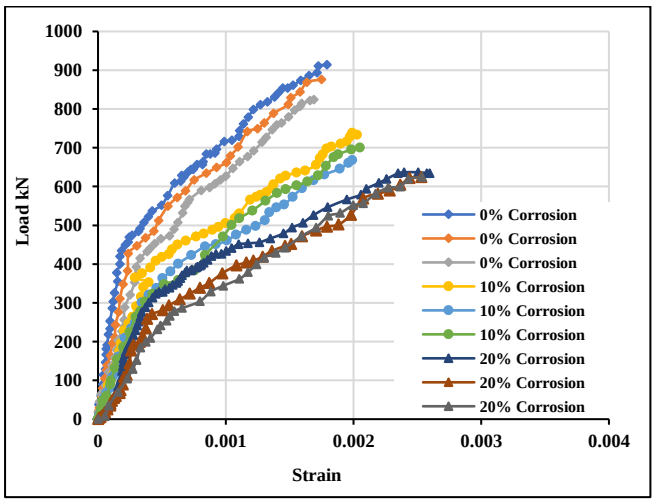

Figure 9. Load – Strain Curve of steel.

The results of each tested column were recorded to generate the curves for that particular group. A data logger was employed

to record signals from the load cell, LVDT, and strain gauges simultaneously.

4. Conclusions

This paper presents experimental investigations to assess the effect of steel rebar corrosion on the behavior of concrete columns. The data collected shows that the average crack width identified in columns was 0.33 mm at a 10% loss and 0.54 mm at a 20% loss. The maximum observed cracking widths corresponded to mass losses of 10% and 20%, with values measured between 0.37 mm and 0.64 mm. Furthermore, the ultimate load capacity decreased by approximately 18.5%-51% for a 10% mass loss and by 25%-65% for a 20% mass loss. Additionally, the longitudinal shortening increased by 33% for a 10% mass loss and by 67% for a 20% mass loss. The strain in the steel bar at mid-span increased by approximately 31% for a mass loss of 10%, and by 55% for a mass loss of 20%.

Author contribution

Shaho Mahmoud Hama supplied materials, conducted the experimental work, prepared the main manuscript text, developed the underlying theory, performed computations, verified analytical methods, investigated and discussed the results, and contributed to the final manuscript preparation.

Ali Hameed Aziz proposed the research problem and suggested the methodology reviewed in the manuscript.

Conflict of interest

The authors declare that there are no conflicts of interest regarding the publication of this manuscript.

Acknowledgement

We extend our sincere thanks to the Head and faculty members of the Civil Engineering Department at Mustansiriyah University for their valuable efforts.

References

[1] J. Y. Hu, S. S. Zhang, E. Chen, and W. G. Li, "A Review on Corrosion Detection and Protection of Existing Reinforced Concrete (RC) Structures," *Construction and Building Materials*, vol. 325, p. 126718, Mar. 2022, doi: https://doi.org/10.1016/j.conbuildmat.2022.126718.

[2] Q. Li, Z. Dong, Q. He, C. Fu, and X. Jin, "Effects of Reinforcement Corrosion and Sustained Load on Mechanical Behavior of Reinforced Concrete Columns," *Materials*, vol. 15, no. 10, p. 3590, May 2022, doi: https://doi.org/10.3390/ma15103590.

[3] J. W. Wright and C. P. Pantelides, "Axial Compression Capacity of Concrete Columns Reinforced with corrosion-resistant Hybrid Reinforcement," *Construction and Building Materials*, vol. 302, p. 124209, Oct. 2021, doi: https://doi.org/10.1016/j.conbuildmat.2021.124209

[4] V. H. Dang and R. François, "Influence of long-term Corrosion in Chloride Environment on Mechanical Behaviour of RC Beam," *Engineering Structures*, vol. 48, pp. 558–568, Mar. 2013, doi: https://doi.org/10.1016/j.engstruct.2012.09.021.

[5] W. Zhu, C. Yang, Z. Yu, J. Xiao, and Y. Xu, "Impact of Defects in Steel-Concrete Interface on the Corrosion-Induced Cracking Propagation of the Reinforced Concrete," *KSCE Journal of Civil Engineering*, vol. 27, no. 6, pp. 2621–2628, Apr. 2023, doi: https://doi.org/10.1007/s12205-023-0458-5.

[6] R. Qian, Q. Li, C. Fu, Y. Zhang, Y. Wang, and X. Jin, "Atmospheric chloride-induced Corrosion of steel-reinforced Concrete Beam Exposed to Real marine environment for 7 Years," *Ocean Engineering*, vol. 286, Part 2, p. 115675, Oct. 2023, doi: https://doi.org/10.1016/j.oceaneng.2023.115675.

[7] V. Q. Dang, Y. Ogawa, P. T. Bui, and K. Kawai, "Effects of Chloride Ions on the Durability and Mechanical Properties of Sea Sand Concrete Incorporating Supplementary Cementitious Materials under an Accelerated Carbonation Condition," *Construction and Building Materials*, vol. 274, p. 122016, Mar. 2021, doi: https://doi.org/10.1016/j.conbuildmat.2020.122016.

[8] H. S. Abdo, A. H. Seikh, J. A. Mohammed, M. Luqman, S. A. Ragab, and S. M. Almotairy, "Influence of Chloride Ions on Electrochemical Corrosion Behavior of Dual-Phase Steel over Conventional Rebar in Pore Solution," *Applied Sciences*, vol. 10, no. 13, p. 4568, Jun. 2020, doi: https://doi.org/10.3390/app10134568.

[9] H. F. Zahid, P. Jiradilok, V. Singh Kuntal, and K. Nagai, "Investigation of the Effects of Multiple and multi-directional Reinforcement on corrosion-induced Concrete Cracking Pattern," *Construction and Building Materials*, vol. 283, p. 122594, May 2021, doi: https://doi.org/10.1016/j.conbuildmat.2021.122594.

[10] Y.-S. Kim, B.-G. Lee, J.-S. Jung, and K.-S. Lee, "Seismic Performance Evaluation of Corrosion-Damaged Reinforced Concrete Columns Controlled by Shear Based on Experiment and FEA," *Materials*, vol. 15, no. 18, p. 6361, Sep. 2022, doi: https://doi.org/10.3390/ma15186361

[11] Y. Ma, Y. Che, and J. Gong, "Behavior of Corrosion-Damaged Circular Reinforced Concrete Columns under Cyclic Loading," *Construction and Building Materials*, vol. 29, pp. 548–556, Apr. 2012, doi: https://doi.org/10.1016/j.conbuildmat.2011.11.002

[12] Q. Li, L. Huang, H. Ye, C. Fu, and X. Jin, "Mechanical Degradation of Reinforced Concrete Columns Corroded under Sustained Loads," *International Journal of Civil Engineering*, vol. 18, no. 8, pp. 883–901, Apr. 2020, doi: https://doi.org/10.1007/s40999-020-00511-w

[13] H. Zhou, Y. Xu, Y. Peng, X. Liang, D. Li, and F. Xing, "Partially Corroded Reinforced Concrete Piers under Axial Compression and Cyclic Loading: an Experimental Study," *Engineering Structures*, vol. 203, pp. 109880–109880, Nov. 2019, doi: https://doi.org/10.1016/j.engstruct.2019.109880

[14] A. Celik, H. Yalciner, A. Kumbasaroglu, and A. İ. Turan, "An Experimental Study on Seismic Performance Levels of Highly Corroded Reinforced Concrete Columns," *Structural Concrete*, vol. 23, no. 1, Jul. 2021, doi: https://doi.org/10.1002/suco.202100065

[15] N. El-Joukhadar, F. Dameh, and Stavroula Pantazopoulou, "Seismic Modelling of Corroded Reinforced Concrete Columns," *Engineering Structures*, vol. 275, no. Part A, pp. 115251–115251, Nov. 2022, doi: https://doi.org/10.1016/j.engstruct.2022.115251

[16] Y. Song, J. Wang, and J. Du, "Experimental Study on Seismic Performance of Partially Corroded Squat RC Shear Walls in Coastal Environment," *Buildings*, vol. 14, no. 2, p. 404, Feb. 2024, doi: https://doi.org/10.3390/buildings14020404

[17] A Bentur, Ns Berke, and S. Diamond, Steel Corrosion in Concrete: Fundamentals and Civil Engineering Practice. CRC Press; 1st Edition, 1997.

[18] American Concrete Institute, "ACI CODE-318-19: Building Code Requirements for Structural Concrete and Commentary," www.concrete.org, 2019. https://www.concrete.org/store/productdetail.aspx?ItemID=318U19&Language=English&Units=US_Units

[19] ASTM A615/ A615M-20, "Specification for Deformed and Plain Carbon-Steel Bars for Concrete Reinforcement," West Conshohocken, PA, USA., 2020, doi: https://doi.org/10.1520/a0615_a0615m-20

[20] Central Organization for Standardization and Quality Control, "Portland Cement," Iraqi Standard specification, No. 5, 2019.

[21] Central Organization for Standardization and Quality Control, Planning Council, Baghdad, IRAQ, "The Used Aggregate from Natural Sources in Concrete and Building," Iraqi Specifications, No.45, 1984.

[22] British, S.116, "Testing concrete-Part 116: Method for Determination of Compressive Strength of Concrete cubes," British Standards Institution, London, UK, 1983.

[23] A. Kramida, K. Olsen, and Y. Ralchenko, "Periodic Table of the Elements," *NIST*, Aug. 05, 2019. https://www.nist.gov/pml/periodic-table-elements

[24] İ. Hocaoğlu, "The Effect of Reinforcement Diameter on Accelerated Corrosion Level in Concretes," *Civil Engineering and Architecture*, vol. 11, no. 2, pp. 1048–1058, Mar. 2023, doi: https://doi.org/10.13189/cea.2023.110237

[25] Z. Ye, W. Zhang, X. Gu, and X. Liu, "Experimental Investigation on Shear Fatigue Behavior of Reinforced Concrete Beams with Corroded Stirrups," *Journal of Bridge Engineering*, vol. 24, no. 2, p. 04018117, Feb. 2019, doi: https://doi.org/10.1061/(asce)be.1943-5592.0001350.

[26] J. Y. Hu, Y. J. Liu, Z. Dong, and S. S. Zhang, "A Novel Method to Measure the Actual Corrosion resistance/rate of Steel Reinforcement during impressed-current Accelerated Corrosion Test," *Construction and Building Materials*, vol. 426, pp. 136060–136060, Apr. 2024, doi: https://doi.org/10.1016/j.conbuildmat.2024.136060.

[27] S. Hong et al., "Determination of Impressed Current Efficiency during Accelerated Corrosion of Reinforcement," *Cement and Concrete Composites*, vol. 108, p. 103536, Apr. 2020, doi: https://doi.org/10.1016/j.cemconcomp.2020.103536

[28] A. Z. Morshed, S. Shakib, and T. Jahin, "Characterization of Impressed Current Technique to Model Corrosion of Reinforcement in Concrete," *Journal of Engineering Science*, vol. 11, no. 1, pp. 93–99, Oct. 2020, doi: https://doi.org/10.3329/jes.v11i1.49551

[29] S. Hong, G. Shi, F. Zheng, M. Liu, D. Hou, and B. Dong, "Characterization of the Corrosion Profiles of Reinforcement with Different Impressed Current Densities by X-ray micro-computed Tomography," *Cement and Concrete Composites*, vol. 109, p. 103583, May 2020, doi: https://doi.org/10.1016/j.cemconcomp.2020.103583